DOI: 10.1002/chem.200701462

Testing Electron Transfer within Molecular Associates Built around Anionic C_{60} and C_{70} Dendrofullerenes and a Cationic Zinc Porphyrin

Ginka H. Sarova,[a] Uwe Hartnagel,[b] Domenico Balbinot,[b] Sevda Sali,[a] Norbert Jux,*[b] Andreas Hirsch,*[b] and Dirk M. Guldi*[a]

Dedicated to Professor Emanuel Vogel on the occasion of his 80th birthday

Abstract: Mono- and bis-functionalized C_{60} and C_{70} fullerene derivatives (**DF**, **1**–**10**) that carry one or two oligoanionic dendritic termini in their malonate addends and an oligocationic octapyridinium zinc porphyrin salt (**ZnP**) were found to self-assemble in buffered aqueous solution to yield a novel series of 1:1 and/or 1:2 electron transfer hybrid associates. Remarkably high association constants—typically on the order of $10^8\ M^{-1}$—were derived that corroborate stable complex formations. A combination of electrostatic and charge-transfer interactions that are operative between the electron-accepting **DF** and the electron-donating **ZnP** is considered to contribute to the uniquely high complex stability. First insight into intracomplex excited state interactions came from steady-state and time-resolved fluorescence quenching experiments that were performed with the molecular **ZnP**/**DF** hybrid associates. Excited state quenching processes are, for example, evident in form of a bi-exponential fluorescence decay of **ZnP**—corresponding to a distribution of associated and non-associated **ZnP**. Unambiguous evidence for an intracomplex electron transfer quenching, namely, formation of $ZnP^{\bullet+}/C_{60}^{\bullet-}$ and $ZnP^{\bullet+}/C_{70}^{\bullet-}$ radical ion pairs, was gathered in time-resolved transient absorption measurements. Lifetimes of these radical ion-pairs range from nanoseconds to a few microseconds.

Keywords: electron transfer · fullerenes · porphyrinoids · time-resolved transient-absorption spectroscopy

Introduction

In the attempt to design highly efficient molecular architectures that give rise to electron donor–acceptor interactions, porphyrins and fullerenes have been widely utilized as effective building blocks as a result of their remarkable electrochemical, chemical, and photophysical properties.[1] Novel organic/inorganic nanocomposites based on water-soluble C_{60} monoadducts emerged, for example, as integrative building blocks in the context of solar-energy conversion and photovoltaics.[2,3]

As the water solubility of fullerene derivatives often goes hand in hand with the presence of a high number of charges, it is quite obvious to employ electrostatic interactions for the construction of supramolecular assemblies. Interestingly, this idea has found widespread attention over the last decade with the use of all kinds of oligoelectrolytes[4]

It has been shown that an electron-transfer process within an intriguing molecular hybrid associate—consisting of a dendritic fullerene oligocarboxylate **1** and an octapyridinium zinc porphyrin (**ZnP**) salt[5]—leads to a remarkably long lifetime of 1.1 μs for an efficiently formed radical ion-pair state.[6,7] Molecular dynamic simulation studies have further underlined that the effective π–π distance between **1** and **ZnP** is approximately 8 Å and that **1** is not able to completely cover **ZnP**, thus leaving approximately half of the **ZnP** unit uncovered and exposed to the solvent (i.e., water). Pronounced electrostatic interactions also govern the association of positively charged proteins (i.e., native iron cyto-

[a] Dr. G. H. Sarova, S. Sali, Prof. Dr. D. M. Guldi
Department of Chemistry and Pharmacy & Interdisciplinary Center for Molecular Materials (ICMM)
University of Erlangen-Nuremberg
Egerlandstrasse 3, 91058 Erlangen (Germany)
Fax: (+49) 9131-8528307
E-mail: dirk.guldi@chemie.uni-erlangen.de

[b] Dr. U. Hartnagel, Dr. D. Balbinot, Dr. N. Jux, Prof. Dr. A. Hirsch
Department of Chemistry and Pharmacy & Interdisciplinary Center for Molecular Materials (ICMM)
University of Erlangen-Nuremberg
Henkestrasse 42, 91054 Erlangen (Germany)
Fax: (+49) 9131-8526864
E-mail: norbert.jux@chemie.uni-erlangen.de
andreas.hirsch@chemie.uni-erlangen.de

Supporting information for this article is available on the WWW under http://www.chemeurj.org/ or from the author.

chrome c and reconstituted zinc cytochrome c) with polyanionic dendrofullerenes (i.e., **1** and **3**); as a consequence, stable protein–fullerene hybrids are formed.[8,9]

Herein, the electron donor–acceptor interactions built around the rigid and highly charged octapyridinium **ZnP** salt are taken to the next level. In particular, a novel series of C_{60} and C_{70} fullerenes **1**–**10**—mono- and bisfunctionalized with dendritic addends (Scheme 1)— were tested. Each of these dendritic addends consisted of one or two building blocks that carried up to nine carboxylic acid groups. pH titrations on dendrofullerenes **1** and **3** showed that the carboxylic acid groups of the Newkome dendrimer branches are almost completely deprotonated at pH≈7.[10] Hence, pH 7 supports effective negative charges of 6 (**4**–**7**), 9 (**1**, **2**, **8**, and **9**), 18 (**3** and **10**) per addend. In addition to the number of charges, the spatial orientation (e.g., see **5**–**7**) was also varied to study the influence of shape on the aggregation and electron-transfer properties. Since the nature of the additional moieties in the side chains can have a substantial effect on the dispersion properties and complexation with the cationic **ZnP** counterpart, we also altered the substituents of the unsymmetrical malonate addends in **1**, **2**, **8**, and **9**. Finally, to investigate the influence of the electronic properties of the fullerene chromophore, we used a selection of different cores either by employing C_{70} as an all-carbon cage (i.e., **8**–**10**) or by establishing three different bisaddition patterns of C_{60} (i.e., **5**–**7**) with slightly different absorption and redox characteristics.

Interestingly, a direct comparison of implementing C_{60} or C_{70} into similar electron donor–acceptor conjugates is limit-

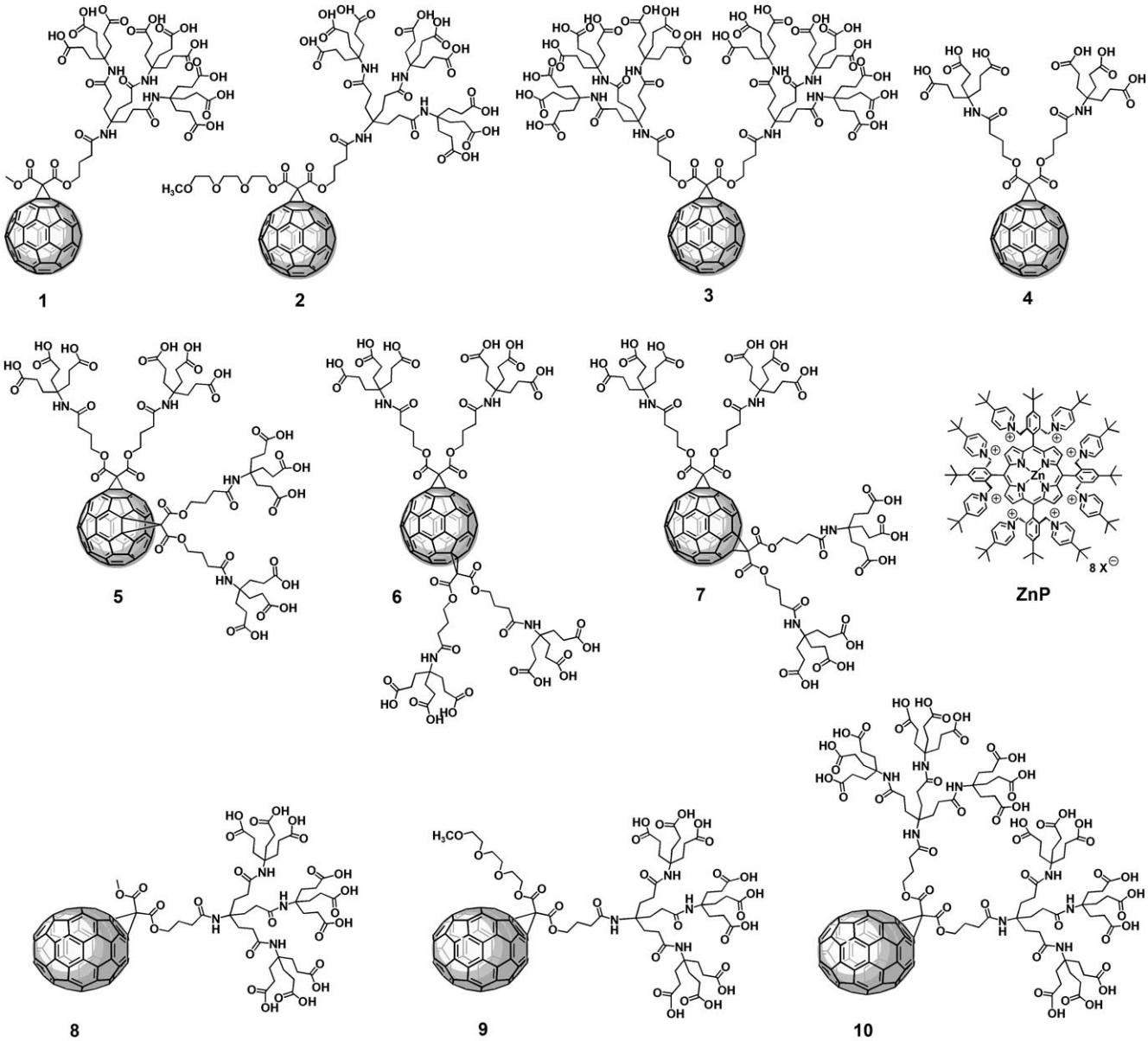

Scheme 1. Water-soluble anionic **DF**s **1**–**10** and octapyridinium **ZnP**.

ed to a few, rare cases. It is important that C_{60} and C_{70} display nearly identical reduction potentials in electrochemical experiments,[11] which also holds for the corresponding derivatives of C_{60} and C_{70} systems.[12] Nevertheless, the initial charge separation was shown to be accelerated when contrasting C_{70}–porphyrin with the corresponding C_{60}–porphyrin.[13,14] A smaller reorganization energy for C_{70} and a different electronic coupling have been considered to explain the observed differences in electron-transfer rates.[13,14]

Results and Discussion

Syntheses of fullerene oligocarboxylic acids 5–10: The dendritic fullerene derivatives **1**,[6] **2**,[15] **3**,[16] and **4**[17] have been prepared previously. As we have shown earlier, the formation of aggregates between **ZnP** and fullerene oligocarboxylates **1**–**3** is governed by the number and spatial arrangement of the charges. Thus, it seemed appropriate to look into C_{60} bisadducts in which the dendritic branches sit in well-defined positions according to the substitution pattern of the fullerene. The reaction of a twofold excess of the G1-subsituted malonate **11** with C_{60} under typical cyclopropanation conditions gave a mixture of the *tert*-butyl ester derivatives *e*-bisadduct **12**, *trans*-2-bisadduct **13**, and *trans*-3-bisadduct **14**, which were separated by HPLC (Scheme 2).

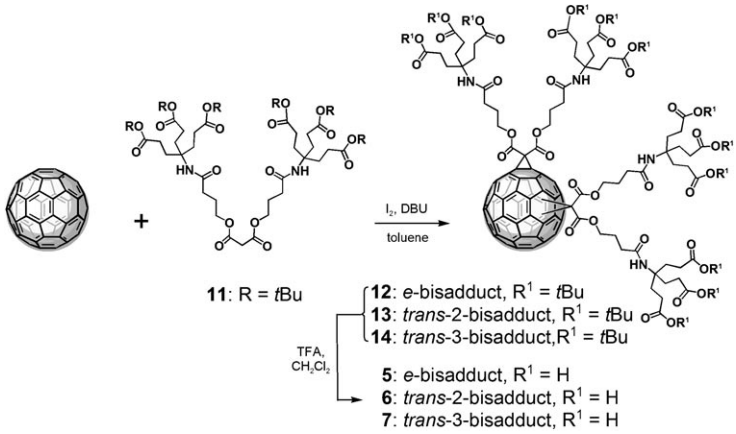

Scheme 2. Syntheses of [60]fullerene dodecacarboxylic acids **5**–**7**. DBU = diaza(1,3)bicyclo[5.4.0]undecane, TFA = trifluoroacetic acid.

The esters **12**–**14** were cleaved with trifluoroacetic acid (TFA), thus liberating the desired [60]fullerene acids **5**–**7**. The assignment of isomers in both series was performed by using ^{13}C NMR spectroscopic analysis (number of signals) and the typical UV/Vis bands for *e*- (C_s symmetry, 29 ^{13}C NMR sp^2 signals, λ_{max} = 422, 483 nm), *trans*-2- (C_2 symmetry, 28 ^{13}C NMR sp^2 signals, λ_{max} = 437, 473 nm), and *trans*-3-bisadducts (C_2 symmetry, 28 ^{13}C NMR sp^2 signals, λ_{max} = 411, 425, 494 nm).

So far, we have looked only into the Coulomb complex formation of C_{60} derivatives. As the C_{70} species possesses different properties and reactivity, we decided to prepare several water-soluble C_{70} derivatives carrying carboxylate groups to allow for electrostatic association with the positively charged **ZnP**. Our studies have revealed that it is of crucial importance to Coulomb complex generation that the inherent self-aggregation of water-soluble fullerenes is suppressed.[15] To get a better understanding of this phenomenon for the [70]fullerene, the C_{70} moiety was treated with three different malonates, that is, the simple monosubstituted malonate **15** carrying a G2-Newkome dendrimer, the triethylene glycol-substituted malonate **16** with the same dendron, and the symmetrical malonate **17** with two G2 arms (Scheme 3).

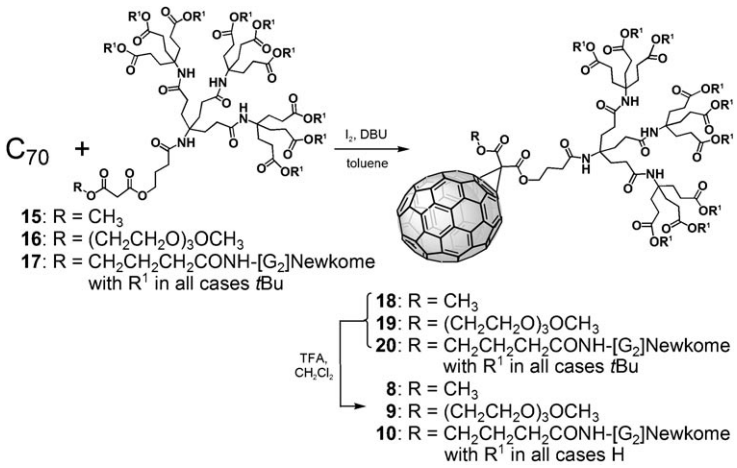

Scheme 3. Syntheses of [70]fullerene oligocarboxylic acids **8**–**10**.

The syntheses of the precursor molecules **18**–**20** followed typical monosubstitution protocols for fullerenes using iodine and DBU. The position of the substituent on C_{70} was determined by comparison with known monoadducts of C_{70}.[18] Finally, the free acids were obtained by acid-promoted saponification of the ester groups of **18**–**20**, which led to the desired carboxylic acids **8**–**10** in quantitative yields. See the Supporting Information for details on the synthesis and characterization of the bisadducts of C_{60} and the monoadducts of C_{70}.

Absorption spectroscopy: The structures of the water-soluble cationic **ZnP** salts and the anionic dendrofullerenes (**DF**s) studied are shown in Scheme 1. Consistent with our previous results,[6] upon adding **1**–**10** to aqueous solutions of **ZnP** a gradual decrease in intensity and a red shift of the absorption bands for the porphyrin unit are observed throughout the visible region of the spectrum. This observation suggests effective interactions between **1**–**10** and **ZnP** in the ground state. The bathochromic shifts scale with the concentration of added fullerene. Common to these titration experiments—C_{60} and C_{70} monoadducts (i.e., **1**, **2**, **8**, and **9**)—is the development of an isosbestic point around 440 nm.[19] The presence of only two absorbing species that are in a dynamic equilibrium is implicit. Indeed, in these as-

semblies, the Job method of continuous variations confirmed the formation of complexes with a 1:1 stoichiometry (see the Supporting Information).[19]

At first glance, similar changes were noted when titrating ZnP with either C_{60}/C_{70} monoadducts **3**, **4**, and **10** carrying two dendritic termini in their malonate addends or with C_{60} bisadducts **5**, **6**, and **7**. However, upon closer analysis, some differences relative to **1**, **2**, **8**, and **9** were noted. More precisely, the appearance of a second isosbestic point (Figure 1) is reproducibly seen. Alternatively, toward the final stage of the titration the spectra fail to go through an isosbestic point at all.

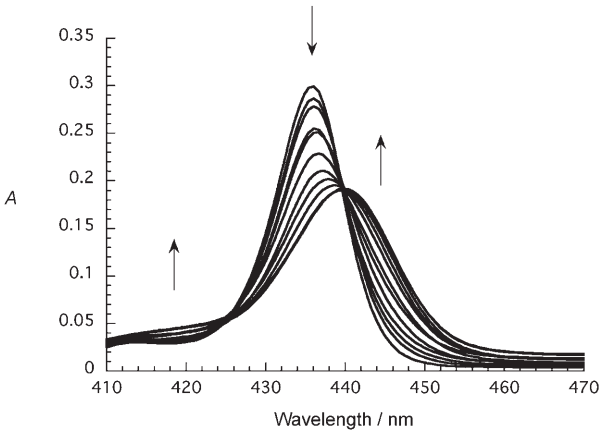

Figure 1. Changes in the **ZnP** Soret band (8.4×10^{-7} M) observed upon adding different concentrations of **10** (6.4×10^{-8}–9×10^{-7} M).

In line with the aforementioned observations, maxima from the Job-plot analysis are seen which are not at 0.5 but at 0.68 for the hybrid assemblies of **ZnP** with **3**, **4**, and **10**.[19] Thus, we postulate complexes in which **ZnP** interacts with these **DF**s in a 2:1 fashion. The analysis becomes even more complicated for **5**–**7**. In these cases, the Job plots displayed one or two maxima depending on the wavelength, at which point data were taken for the analysis. A possible interpretation involves complexes that have different stoichiometries and that are present in equilibrium.[19]

The formation of 1:1, or 1:1 along with 2:1, complexes between **ZnP** and the anionic dendrofullerenes **2** and **3** has been shown previously in electrophoresis experiments.[15] Whereas **ZnP** and cytochrome c were shown to form 1:1 complexes with **2**, the results displayed a clear formation of both 1:1 and 2:1 complexes with **3**.

Steady-state fluorescence: For example, in steady-state fluorescence experiments the changes of the fluorescence intensity of **ZnP** were followed upon addition of increasing quantities of **DF**s (only buffered solutions of **ZnP** (pH 7.2, 0.05 M KH_2PO_4) were used). Quite drastic quenching of the porphyrin emission—typically seen to evolve during these titration experiments—is tentatively attributed to originate from electron-transfer processes between the photoexcited ZnP and the DF ground state. An illustration is given in Figure 2, which represents the spectral changes in conjunction with the ZnP fluorescence in the absence and presence of variable concentrations of **2**. For all the C_{60} and C_{70} monoadducts, a saturation point of the quenching correlation was reached after adding just one equivalent of the fullerene; here, the donor fluorescence quenching is quantitative (i.e., 99%). On the other hand, for the C_{60} bisadducts to reach the plateau value fullerene concentrations that exceeded 1.5 equivalents were needed. We used the fluorescence quantum yields at the plateau values in the next step to evaluate the dynamics of the excited-state deactivation process. For example, the efficient quenching of the fluorescence in **ZnP/2** leads to a fast electron-transfer rate of 4.8×10^{10} s^{-1} relative to the intrinsic decay of the singlet excited state of **ZnP**, namely, an intersystem crossing with a rate constant of 3.5×10^{8} s^{-1}.

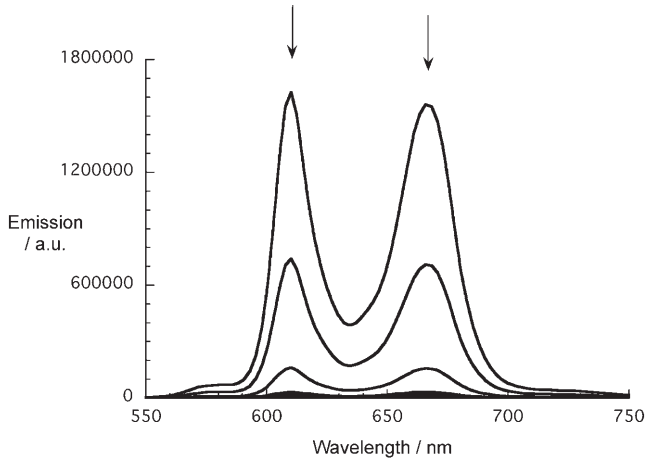

Figure 2. Changes in the steady-state fluorescence of **ZnP** (5.3×10^{-7} M) observed upon adding different concentrations of **2** (0–9.8×10^{-7} M).

The gradual quenching of the steady-state fluorescence intensity of **ZnP** was further used to quantify the association between the cationic **ZnP** and the anionic **DF** species. Data were taken at 610 nm and plotted versus the fullerene concentration. A nonlinear curve fitting according to Equation (1) allowed the association constants to be estimated (Figure 3).

$$\frac{I_F}{I_0} = 1-\frac{1}{2c_D}\left[\frac{1}{K_S}+c_0+c_D-\sqrt{\left(\frac{1}{K_S}+c_0+c_D-4c_0c_D\right)}\right] \quad (1)$$

where I_o refers to the initial fluorescence intensity, c_o is the total porphyrin concentration, c_D is the total concentration of the added fullerene, and K_S is the association constant.

The association constants obtained from the emission titration experiments are summarized in Table 1. Overall, remarkably high association constants were obtained for the assemblies, with **2** displaying the highest values, namely, 3.2×10^{8} M^{-1}. As far as the 2:1 associates are concerned, only

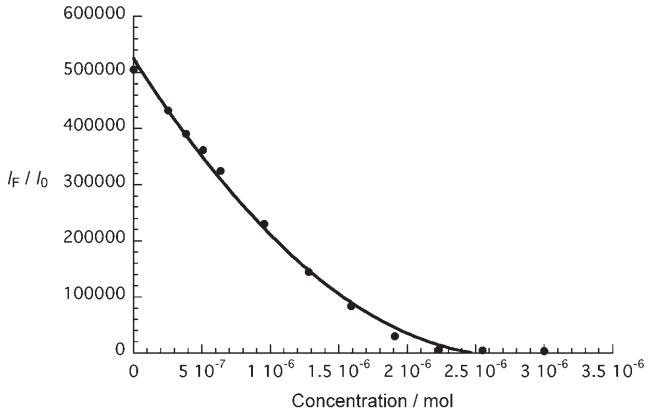

Figure 3. Fluorescence intensity at 610 nm of **ZnP/2**. The concentration of **2** varies from 0 to 3×10^{-6} M, while the **ZnP** concentration is constant at 1.8×10^{-6} M. The solid line corresponds to a fit according to Equation (1), thus giving $K_S = 3.2\times10^{8}\,M^{-1}$.

Table 1. Association constants obtained from steady-state fluorescence titration experiments for 1:1 complex formation between **ZnP** and the studied **DF**s.[a]

Compound	K_S [$10^8\,M^{-1}$]			
	0.05 M KH_2SO_4	0.034 M Na_2SO_4[b]	0.1 M NaCl[b]	0.17 M NaCl[b]
1	0.5[c]			
2	3.2	–	–	–
3	1.0	0.5	0.3	0.1
4	1.3	–	–	–
5	1.8	1.3	0.9	0.6
6	1.9	–	–	–
7	2.1	–	–	–
8	1.9	–	–	–
9	1.1	–	–	–
10	2.3	–	–	–

[a] The estimated values remained constant for ZnP concentrations, which varied from 5×10^{-8} M to 5×10^{-6} M. [b] Buffered with 0.05 M KH_2SO_4. [c] Ref. [6].

the 1:1 complex formation was considered during the evaluation of the experimental data. Estimation of the K_1 and K_2 values was, however, impossible since only the changes that were associated with the ZnP fluorescence were followed.

To test the influence of the ionic strength on the **ZnP/DF** association, we carried out the same titration experiments in the presence of Na_2SO_4 and NaCl at different concentrations. As expected and previously confirmed for the **ZnP/1** assembly,[6] an increase in the ionic strength weakens the association between **ZnP** and **DF** (Table 1). Interestingly, the presence of Cl^- ions evokes smaller association constants when compared to, for example, the values obtained in the presence of SO_4^{2-} ions. We assume that as the NaCl concentration increases the HPO_4^- and $H_2PO_4^-$ counteranions of the buffer are replaced in an equilibrium process by Cl^- ions. As these are less strongly bound, the effective charge of the solvated porphyrin increases, thus making the Coulomb complex formation with the negatively charged fullerenes much more likely.

Time-resolved fluorescence: Quenching of the porphyrin emission became also evident in the time-resolved fluorescence experiments. Whereas the fluorescence decay of **ZnP** in the absence of any **DF** is exclusively monoexponential—with an intrinsic lifetime of 2.05 ns—the decays were best fitted upon addition of **DF** by a biexponential fitting function (i.e., a fast-decaying and a slow-decaying component). From the fast-decaying component—attributed to the associated **ZnP/DF** hybrids—the rates for the intracomplex electron-transfer processes were estimated according to Equation (2):

$$k_q = \frac{1}{\tau_1} - \frac{1}{\tau_0} \qquad (2)$$

where τ_o refers to the **ZnP** fluorescence lifetime and τ_1 is the lifetime of the faster-decaying component in the biexponential fitting function. As a leading example, the titration of **ZnP** with **2** should be considered, in which biexponential decays of the **ZnP** fluorescence with lifetimes of 2.05 and 0.07 ns are seen throughout the titrations (Table 2). It is important that the relative weight of the long-lived component decreases throughout the titration and that only the short-lived component is detectable at the plateau of the steady-state fluorescence quenching. Although the obtained lifetime of 0.07 ns is in a good agreement with the electron-transfer rate estimated from the steady-state fluorescence spectra, we must point out that this value is essentially the time resolution of our apparatus. Still, it signifies that electron-transfer rates faster than $1\times10^{10}\,s^{-1}$ should be expected.

Table 2. Fluorescence lifetimes and rate constants for the quenching process obtained from time-resolved fluorescence decays.

Compound	τ_o [ns][a]	τ_1 [ns][b]	k_q [s^{-1}][c]	Intrinsic lifetimes [ns]
ZnP	2.05	–		2.8
1	2.30	0.06	1.68×10^{10}	0.080
2	2.05	0.07	1.49×10^{10}	0.114
3	2.05	0.09	1.03×10^{10}	0.120
4	2.10	0.10	9.52×10^{9}	–
5	2.10	0.11	8.45×10^{9}	0.170
6	2.15	0.22	4.10×10^{9}	–
7	2.05	0.17	5.26×10^{9}	–
8	2.20	0.16	5.72×10^{9}	0.250
9	2.40	0.19	4.85×10^{9}	0.270
10	2.30	0.17	5.41×10^{9}	–

[a] Corresponds to the fluorescence lifetimes of **ZnP**. [b] Corresponds to the fluorescence lifetimes of **ZnP/DF** hybrids. [c] Obtained according to Equation (2).

Transient-absorption spectroscopy: Transient-absorption spectroscopy provided support for the proposed electron-transfer mechanism and gave conclusive information about the quenching pathways and the corresponding photoproducts.

ZnP reference compound: Figure 4 illustrates that two transients that correspond to the ^{1}ZnP* and ^{3}ZnP* excited states are discernable on the femto-, pico-, and nanosecond timescales. The first transient, namely, the singlet excited state of **ZnP**, ^{1}ZnP*, appears simultaneously with the conclusion of the femtosecond laser pulse and is characterized by an absorption band that is centered at approximately 470 nm and a broad and low-intensity absorption in the range 600–700 nm, with two minima in the Q-band region. Figure 4a exemplifies the spectral changes associated with the **ZnP** singlet excited-state formation. The singlet excited state of **ZnP** is short-lived (i.e., the intrinsic lifetime is 2.8 ns), since it undergoes fast and efficient intersystem crossing to the corresponding triplet manifold. The latter is seen on the picosecond timescale as a slowly evolving species for which a maximum is registered at 840 nm (Figure 4a). Moreover, it is readily observed on the nanosecond timescale, as is corroborated in Figure 4b. The triplet lifetime of 450 μs, determined in our experiment, agrees well with the previously reported data.[20]

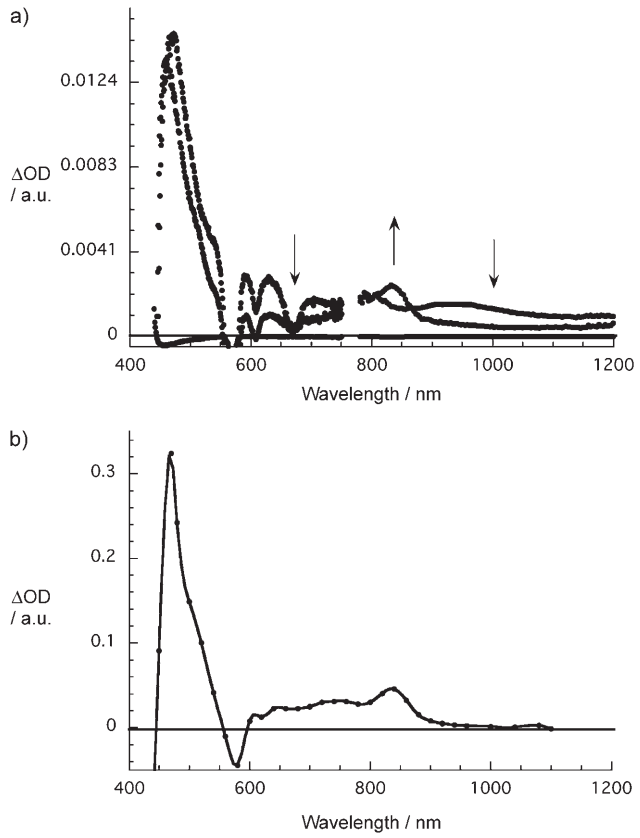

Figure 4. a) Differential absorption changes obtained upon femtosecond flash photolysis (570 nm) of **ZnP** (8×10^{-5} M) in an argon-saturated buffer solution (pH 7.2) with different time delays between 0 and 2892 ps at room temperature (arrows indicate the evolution of differential changes). b) Differential absorption changes recorded with a time delay of 8.93×10^{-6} s after 355-nm nanosecond photolysis of **ZnP** (4×10^{-5} M)

ZnP/DF assemblies: The observed changes upon femtosecond photolysis with 570-nm excitation of all the C_{60} monoadducts containing hybrid assemblies include fast development of the absorption at 470 nm.[19] This maximum starts, after reaching a maximum at around 0.5 ps, to decay following monoexponential kinetics. Fitting the data gives a lifetime for **ZnP/2** of 114 ps. With the decay of the absorption at 470 nm, the characteristic spectral features[21] of the one-electron oxidized ZnP radical cation ($ZnP^{\bullet+}$) and the one-electron reduced fullerene radical anion ($C_{60}^{\bullet-}$) at 640 and 1020 nm, respectively, appear. Both absorptions are stable on the picosecond timescale and only start to decay in the nanosecond time regime.

In complementary nanosecond transient-absorption experiments performed with 355-nm excitation of 1:1 mixtures of **1**–**4** and **ZnP**, the spectral features show the instantaneous formation of the $ZnP^{\bullet+}/C_{60}^{\bullet-}$ radical ion-pair state; the latter is characterized by absorption features at 640 and 1000 nm.[19] Importantly, no triplet–triplet absorptions, characteristic of either **ZnP** or **DF** units, were observed at 840 and 700 nm, respectively. These observations indicate that an electron-transfer process takes place exclusively from the singlet state of **ZnP** and that the decay of the radical ion pair leads to the direct recovery of the ground state rather than going through an intermediate triplet excited state. The $ZnP^{\bullet+}/C_{60}^{\bullet-}$ radical ion-pair state decays with a lifetime on the scale of microseconds. Table 3 summarizes the data obtained from the nanosecond photolysis for all the assemblies.

Figures 5 and 6 confirm that femto- and nanosecond photolysis also provided support for the electron-transfer mechanism within the hybrid assemblies containing the C_{60} bisadducts **5**–**7**. In particular, femtosecond excitation into the porphyrin Q band at 570 nm of **ZnP/5** led to the features known to correspond to the $C_{60}^{\bullet-}$ and $ZnP^{\bullet+}$ radical ions at 1060 and 640 nm, respectively, as they evolve during the decay of the initially formed absorption of **ZnP** at 470 nm. Again, this decay is best fitted by a monoexponential fitting function with a lifetime of 170 ps, which underpins the elec-

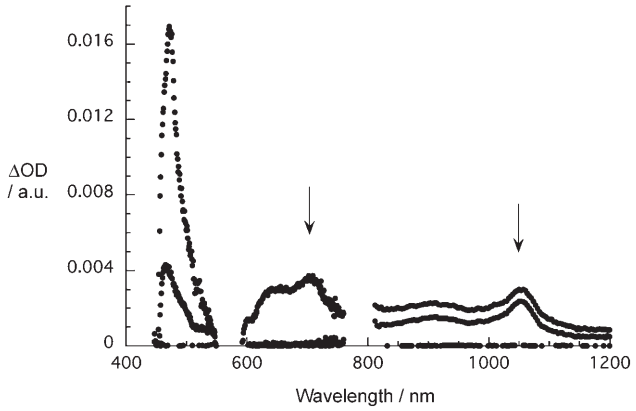

Figure 5. Differential absorption spectrum obtained upon femtosecond flash photolysis (570 nm) of **ZnP/5** in an argon-saturated buffer solution (pH 7.2) with time delays between 0 and 1000 ps at room temperature.

Table 3. Absorption maxima and lifetimes of the $\mathbf{ZnP}^{\bullet+}/\mathbf{DF}^{\bullet-}$ radical ion pair obtained from nanosecond photolysis.

Compound	λ_{max} [nm]	τ [s]
1	1040[a]	1.1×10^{-6}[a]
2	1020	6.5×10^{-6}
3	1000	7.0×10^{-6}
4	1000	4.4×10^{-6}
5	1060	7.5×10^{-6}
6	880	7.2×10^{-6}
7	900	6.2×10^{-6}
8	1350	7.8×10^{-7}
9	1350	5.6×10^{-7}
10	1350	7.4×10^{-7}

[a] Ref. [6].

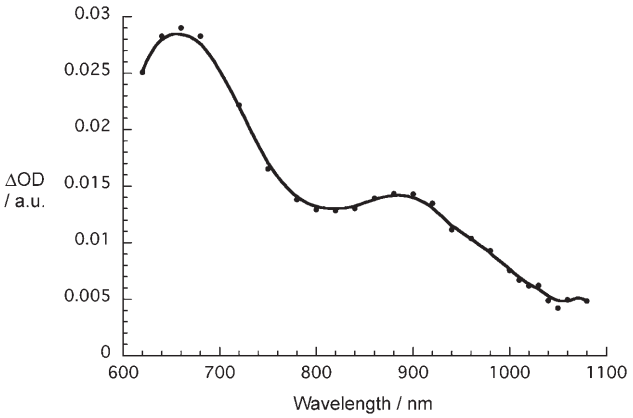

Figure 6. Differential absorption changes obtained upon nanosecond flash photolysis (355 nm) of **ZnP/6** in a nitrogen-saturated buffer solution (pH 7.2) with a time delay of 5×10^{-7} s at room temperature.

tron-transfer rate from the **ZnP** lowest-excited singlet state. In the complementary nanosecond transient absorption measurements, the lifetime of the $ZnP^{\bullet+}/C_{60}^{\bullet-}$ radical ion-pair state was determined to be 7.5 μs.

The differential absorption changes of the C_{70}-containing assemblies **8**–**10**, displayed representatively in Figure 7, were

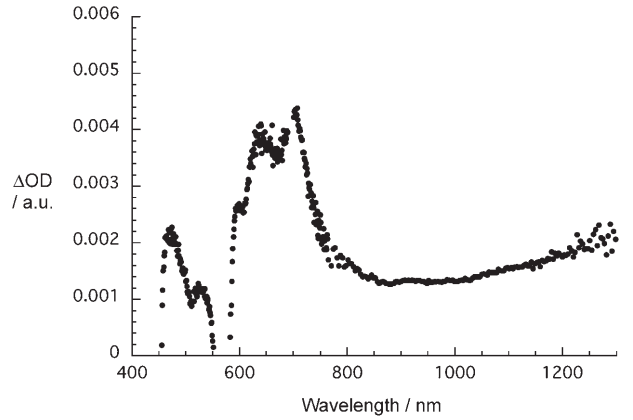

Figure 7. Differential absorption changes obtained upon femtosecond flash photolysis (570 nm) of **ZnP/8** in an argon-saturated buffer solution (pH 7.2) with a time delay of 250 ps at room temperature.

obtained upon femtosecond photolysis (i.e., 570-nm excitation). Similar to the assemblies with the C_{60} mono- and bisadducts, the observed changes involve the fast development of the absorption at 470 nm, characteristic for the ^{1}ZnP* state, which starts to decay following monoexponential kinetics after reaching a maximum (i.e., at 0.4 ps). Fitting the data gives a lifetime for **ZnP/8** of 250 ps. Simultaneously, as the decay of the absorption at 470 nm is observed, the characteristic spectral features of the $ZnP^{\bullet+}$ radical cation at, for example, 640 nm are discernable. Although we were not able to observe the one-electron reduced C_{70} radical anion ($C_{70}^{\bullet-}$) during the femtosecond photolysis experiment, as its absorption is known to maximize at 1350 nm[22] which is near the detection limit of our femtosecond transient apparatus, it is clearly distinguishable (Figure 7).

Both the characteristic absorption bands of the $ZnP^{\bullet+}$ and $C_{70}^{\bullet-}$ radical ions are clearly seen in the nanosecond transient absorption spectrum (Figure 8). Once again, no triplet–

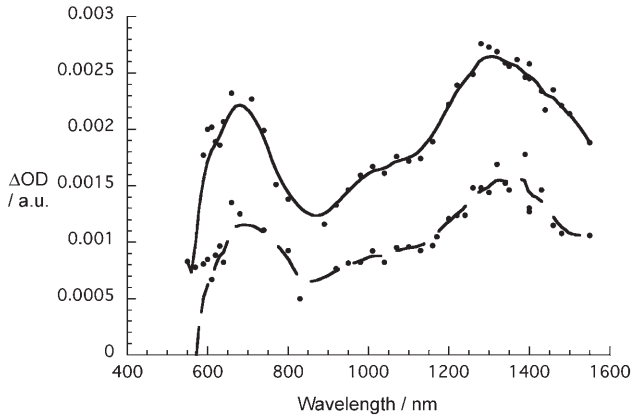

Figure 8. Differential absorption changes obtained upon nanosecond flash photolysis (355 nm) of **ZnP/9** in nitrogen-saturated D_2O (pH 7.2) with time delays of 6×10^{-8} (dashed line) and 1.9×10^{-7} s (solid line) at room temperature.

triplet absorptions, characteristic of either **ZnP** or C_{70} monoadducts, were observed, for example, at 840 or 1100 nm. Table 3 summarizes the data from the nanosecond transient absorption for the **ZnP**/C_{70} assemblies. In contrast to the $ZnPC^{\bullet+}/C_{60}^{\bullet-}$ radical ion-pair, the lifetimes of the $ZnPC^{\bullet+}/C_{70}^{\bullet-}$ radical ion-pair states are only in the range of hundreds of nanoseconds.

Conclusion

Our study indicates that stable complexes ($K_S\approx10^8\,M^{-1}$) are formed between cationic zinc porphyrins and anionic dendrofullerenes as a class of functional fullerodendrimer.[23] The complex formation is driven by electrostatic interactions between oppositely charged species, that is, polyanionic **DF** and polycationic **ZnP**. Charge-transfer interactions also are considered to contribute to the overall complex sta-

bility, as evidenced from the observed red shift of the porphyrin absorption in the visible range of the solar spectrum. The stoichiometry of porphyrin/DF in the complexes was determined to be 1:1 and 2:1 for the different assemblies. For the C_{60} bisadducts, complexes of different stoichiometry are formed. The highest K_S values arose from the C_{60} and C_{70} monoadducts with the polyethylene glycol chain. Interestingly, the binding is not very specific as the correlation between the total number of carboxylate groups (i.e., 9 in **1**, **2**, **8**, and **9**; 18 in **3** and **10**; 6 in **4**; and 12 in **5**, **6**, and **7**) and the K_S values reflects. In other words, this relationship corroborates earlier molecular dynamic simulations,[6] which suggested that as soon as one salt bridge is formed the other bridges are built quickly, thus leading to a structure in which the **DF** covers about one half of the **ZnP** unit.

The transient-absorption experiments show that the singlet excited-state features of **ZnP** decay through an intermolecular charge-transfer reaction to form the corresponding radical ion-pair states (Scheme 4). Notable differences are seen for the different classes of electron acceptors (i.e., mono- and bisfunctionalized C_{60} and C_{70} derivatives). The fastest charge separation occurs for the monofunctionalized C_{60} derivatives, while the more negative reduction potentials of the bisfunctionalized C_{60} derivatives leads to a slowing down of the charge-transfer processes. The dynamics associated with the monofunctionalized C_{70} derivatives fall, however, in between those dynamics of the bisfunctionalized C_{60} derivatives. This finding is surprising since their first reduction potentials are nearly identical to those potentials determined for the analogous C_{60} derivatives. Spectroscopically, the formation of the radical ion-pair was monitored by spectral features that developed in parallel to the disappearance of the **ZnP** singlet–singlet absorption. These features are, in particular, a one-electron oxidized radical cation absorption of **ZnP** in the visible region (i.e., 600–800 nm) and a one-electron reduced radical anion absorption of C_{60}/C_{70} in the near-infrared region (i.e., 900–1400 nm).

All of the radical ion-pair states decay to their singlet ground states, without passing through the intermediate triplet excited states of **ZnP**, C_{60}, or C_{70}. Notably, the decays of the radical ion-pair state for C_{60} assemblies are seen within a few microseconds, whereas the decays are completed within a few hundreds of nanoseconds for the analogous C_{70} assemblies.

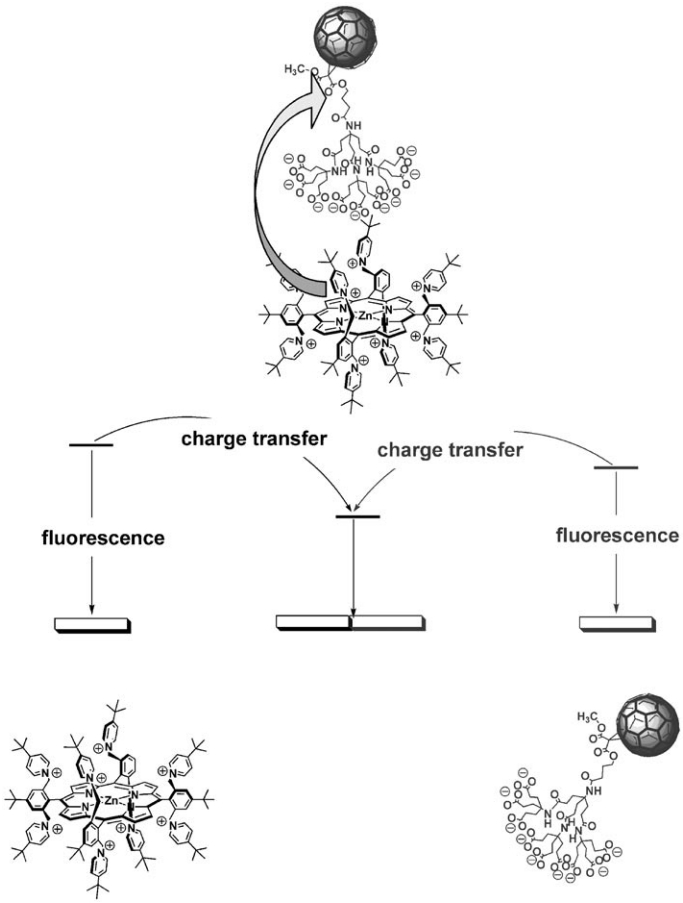

Scheme 4. Excited-state interactions in **ZnP** (left), **DF** (right), and **ZnP**/**DF** (center).

Acknowledgements

This work was supported by the Deutsche Forschungsgemeinschaft (SFB 583, Ju323/5–1), FCI, and the Office of Basic Energy Sciences of the US Department of Energy.

[1] K. M. Kadish, K. M. Smith, R. Guilard, *The Porphyrin Handbook*, Academic Press, San Diego, **2000**.
[2] D. M. Guldi, I. Zilbermann, A. Lin, M. Braun, A. Hirsch, *Chem. Commun.* **2004**, 96.
[3] D. M. Guldi, I. Zilbermann, G. A. Anderson, A. Lin, D. Balbinot, N. Jux, M. Hatzimarinaki, A. Hirsch, M. Prato, *Chem. Commun.* **2004**, 726.
[4] a) X. Arys, A. M. Jonas, A. Laschewsky, R. Legras in *Supramolecular Polymers* (Ed.: A. Cifferi), Marcel Dekker, New York **2000**, p. 505; b) P. Bertrand, A. M. Jonas, A. Laschewsky, R. Legras, *Macromol. Rapid Commun.* **2000**, *21*, 319; c) X. Arys, P. Fischer, A. M. Jonas, M. M. Koetse, A. Laschewsky, R. Legras, E. Wischerhoff, *J. Am. Chem. Soc.* **2003**, *125*, 1859; d) I. Ruhlmann, J. Zimmermann, W. Fudickar, U. Siggel, J.-H. Fuhrhop, *J. Electroanal. Chem.* **2001**, *503*, 1; e) G. Li, W. Fudickar, M. Skupin, A. Klyszcz, C. Draeger, M. Lauer, J.-H. Fuhrhop, *Angew. Chem.* **2002**, *114*, 1906; *Angew. Chem. Int. Ed.* **2002**, *41*, 1828; f) W. Fudickar, J. Zimmermann, L. Ruhlmann, J. Schneider, B. Roeder, U. Siggel, J.-H. Fuhrhop, *J. Am. Chem. Soc.* **1999**, *121*, 9539; g) B. Hamelin, L. Jullien, C. Derouet, C. H. du Penhoat, P. J. Berthault, P. *J. Am. Chem. Soc.* **1998**, *120*, 8438; h) L. Jullien, H. Cottet, B. Hamelin, A. Jardy, *J. Phys. Chem. B* **1999**, *103*, 10866; i) L. P. Balogh, S. M. Redmond, P. Balogh, H. Tang, D. C. Martin, S. C. Rand, *Macromol. Biosci.* **2007**, *7*, 1032; j) Q. Zhang, L. Zhang, J. Li, *J. Phys. Chem. C* **2007**, *111*, 8655; k) K. Y. K. Man, C. W. Tse, K. W. Cheng, A. B. Djurisic, W. K. Chan, *J. Inorg. Organomet. Pol. Mater.* **2007**, *17*, 223.
[5] N. Jux, *Org. Lett.* 2000, ***2***, 2129–2132.
[6] D. Balbinot, S. Atalick, D. M. Guldi, M. Hatzimarinaki, A. Hirsch, N. Jux, *J. Phys. Chem. B* **2003**, *107*, 13273.
[7] D. M. Guldi, M. Prato, *Chem. Commun.* **2004**, 2517.
[8] M. Braun, S. Atalick, D. M. Guldi, H. Lanig, M. Brettreich, S. Burghardt, M. Hatzimarinaki, E. Ravanelli, M. Prato, R. van Eldik, A. Hirsch, *Chem. Eur. J.* **2003**, *9*, 3867.
[9] D. M. Guldi, I. Zilbermann, M. Hatzimarinaki, A. Hirsch, *Z. Phys. Chem.* **2006**, *220*, 487.

[10] M. Brettreich, PhD Thesis, University of Erlangen-Nuremberg, **2000**.
[11] a) P.-M. Allemand, A. Koch, F. Wudl, Y. Rubin, F. Diederich, M. M. Alvarez, S. J. Anz, R. L. Whetten, *J. Am. Chem. Soc.* **1991**, *113*, 1050; b) C. Boudon, J.-P. Gisselbrecht, M. Gross, A. Herrmann, M. Rüttimann, J. Crassous, F. Cardullo, L. Echegoyen, F. Diederich, *J. Am. Chem. Soc.* **1998**, *120*, 7860.
[12] a) F. Cardulo, P. Seiler, L. Isaacs, J.-F. Nierengarten, R. F. Haldimann, F. Diederich, T. Mordasini-Denti, W. Thiel, C. Boudon, J.-P. Gisselbrecht, M. Cross, *Helv. Chim. Acta* **1997**, *80*, 343; b) J.-F. Nierengarten, A. Herrmann, R. R. Tykwinski, M. Rüttimann, F. Diederich, C. Bondon, J.-P. Gisselbrecht, M. Cross, *Helv. Chim. Acta* **1997**, *80*, 293.
[13] H. Imahori, Y. Sakata, *Eur. J. Org. Chem.* **1999**, 2445.
[14] K. Tamaki, H. Imahori, Y. Nishimura, I. Yamazaki, A. Shimomura, T. Okada, Y. Sakata, *Chem. Lett.* **1999**, 227.
[15] U. Hartnagel, D. Balbinot, N. Jux, A. Hirsch, *Org. Biomol. Chem.* **2006**, *4*, 1785.
[16] M. Brettreich, A. Hirsch, *Tetrahedron Lett.* **1998**, *39*, 2731–2734.
[17] P. Witte, F. Beuerle, U. Hartnagel, R. Lebovitz, A. Savouchkina, S. Sali, D. Guldi, N. Chronakis, A. Hirsch, *Org. Biomol. Chem.* in press.
[18] A. Hirsch, M. Brettreich, *Fullerenes – Chemistry and Reactions*, Wiley-VCH, **2005**.
[19] See the Supporting Information for further details.
[20] S. L. Murov, I. Carmichael, G. L. Hug, *Handbook of Photochemistry*, Marcel Dekker, New York, **1993**.
[21] a) D. M. Guldi, H. Hungerbühler, K.-D. Asmus, *J. Phys. Chem. B* **1999**, *103*, 1444; b) D. M. Guldi, H. Hungerbühler, K.-D. Asmus, *J. Phys. Chem.* **1995**, *99*, 9380; c) D. M. Guldi, M. Prato, *Acc. Chem. Res.* **2000**, *33*, 695; d) S. Fukuzumi, H. Imahori, H. Yamada, M. E. El-Khouly, M. Fujitsuka, O. Ito, D. M. Guldi, *J. Am. Chem. Soc.* **2001**, *123*, 2571.
[22] C. A. Reed, R. D. Bolskar, *Chem. Rev.* **2000**, *100*, 1075.
[23] a) J. F. Nierengarten, *Top. Curr. Chem.* **2001**, *217*, 51; b) J.-F. Nierengarten, N. Armaroli, G. Accorsi, Y. Rio, J.-F. Eckert, *Chem. Eur. J.* **2003**, *9*, 36; c) M. Gutierrez-Nava, G. Accorsi, P. Masson, N. Armaroli, J.-F. Nierengarten, *Chem. Eur. J.* **2004**, *10*, 5076; d) U. Hahn, J. J. González, E. Huerta, M. Segura, J.-F. Eckert, F. Cardinali, J. de Mendoza, J.-F. Nierengarten, *Chem. Eur. J.* **2005**, *11*, 6666; e) J.-F. Nierengarten, U. Hahn, A. Trabolsi, H. Herschbach, F. Cardinali, M. Elhabiri, E. Leize, A. Van Dorsselaer, A.-M. Albrecht-Gary, *Chem. Eur. J.* **2006**, *12*, 3365; f) J.-F. Nierengarten, *Chem. Eur. J.* **2000**, *6*, 3667; g) U. Hahn, F. Cardinali, J.-F. Nierengarten, *New J. Chem.* **2007**, *31*, 1128; h) Y. Rio, G. Accorsi, H. Nierengarten, J.-L. Rehspringer, B. Hönerlage, G. Kopitkovas, A. Chugreev, A. Van Dorsselaer, N. Armaroli, J.-F. Nierengarten, *New J. Chem.* **2002**, *26*, 1146; i) T. M. Figueira-Duarte, A. Gégout, J.-F. Nierengarten, *Chem. Commun.* **2007**, 109.

Received: September 14, 2007
Published online: February 1, 2008

